Contribution of one-phonon processes to the electronic energy transfer in disordered solids

A. J. García-Adeva and D. L. Huber
Department of Physics, University of Wisconsin, Madison, Wisconsin 53706
(Received 23 December 1999)

The contribution of nonresonant one phonon processes to the ensemble averaged probability that an initially excited donor is excited at a later time t has been evaluated. A distribution of energy differences between the electronic levels involved in the transfer process is explicitly allowed in this model, which leads to a dependence of the ensemble-averaged probability on the initial distribution of donor ions and on the temperature. In order to perform such an ensemble average, the truncated cumulant expansion method has been used, which has been shown to give an accurate value for this quantity in the experimental time scale. We find that two temporal regimes emerge from the calculation, which are characterized by very distinct temporal, temperature, and initially excited donor ion energy difference dependencies.

I. INTRODUCTION

One of the most interesting problems physics has faced is the determination of the structure of real materials, and it still remains one of the most active fields of research, not only in physics, but also in chemistry, biology, and engineering.

In this sense, optical studies of electronic energy transfer (EET) have shown to be very valuable tools, making it possible to probe the structure of materials to the molecular level (see Ref. 1 and references therein). These kinds of techniques are of special interest in the development of tunable solid-state lasers, optical fibers, probing the structural properties of polymers composites, or studying the first stages of the photosynthesis in biological systems, to quote some examples (see Ref. 2 and references therein).

For this reason, the understanding of the mechanisms involved in the processes of EET between optically active ions (OAI) in solids, in both restricted and unrestricted geometries, is a fundamental problem which has generated renewed interest during recent years.

However, in spite of the abundant literature concerning experimental studies of these processes, the theoretical situation is not so clear and, in fact, it appears that the vast majority of the models used to interpret experimental data share some hypotheses that reduce their range of applicability to homogeneously-broadened transitions, and so they are able to explain only one kind of the EET processes present in a solid, the so-called, non radiative resonant EET processes.

To be more explicit, the transfer of electronic excitation among fluorescent chromophores is explained in terms of nonradiative resonant dipolar interactions between them, following the model earlier introduced by Förster,[3] which can be analytically solved for perfect crystals. In order to generalize the Förster model to include the spatial disorder present in disordered solids, the so-called cumulant expansion method[4–8] was introduced, which allows one to evaluate the configurational average of the probability that an initially-excited chromophore, the so-called donor, remains excited at a later time t, the so-called survival probability, which is a quantity that can be readily compared to fluorescence line narrowing (FLN) experimental data.

This technique has been successfully applied to a variety of both finite and infinite systems with low concentration of OAI.[9–12] The main advantage of this method is its mathematical simplicity; despite the simplicity it provides an accurate description of the survival probability[2,10] in the time scale of experiments, if compared with other mathematically more complicated techniques that take into account the n-body transfer problem, as does, for example, the Gochanour, Andersen, and Fayer diagrammatic theory.[9]

All the aforementioned works share the hypothesis that the main mechanism of the transfer is the resonant dipolar coupling between the chromophores. However, it is well-established that in disordered solids, the energy levels of the chromophores vary from site to site, due to the spatial disorder, which gives rise to a distribution of the radiative transition energies through the solid, leading to the very broad, inhomogeneously-broadened optical spectral lines experimentally observed, but not accounted for in the Förster model.

In the solid there are phonons which play an important role in the dynamics of the transfer, as they can make up the energy difference between the levels involved in the transfer process,[13] giving rise to the so-called nonresonant EET. These processes are characterized by a temperature dependence, in contrast to the resonant EET processes, which are independent of temperature at low temperature. The temperature dependence of the EET provides an additional valuable tool in the determination of the processes involved in the optical excitation migration through the solid, and is a feature that any model which tries to give a general description of the problem not only at 0 K, but also at the finite temperatures, has to deal with.

Recently, this problem has been addressed by Martín and co-workers,[14] and by Lavín and co-workers,[15] who have applied the truncated cumulant expansion to the description of FLN experiments, both in Yb^{3+} fluoroindate-doped glasses and in Eu^{3+} calcium diborate glasses, by assuming that the EET is dominated by one-phonon assisted processes. These authors find a good agreement between the theoretical results and their experimental data. However, their model is not complete, as they only take into account the contribution to the EET of those phonons of very short wavelength, that is, their model is only applicable when the energy mismatch between the OAI is very large. For an inhomogeneously-broadened transition, ions with a small energy mismatch can

also give a significant contribution to the transfer. Moreover, analytical expressions of the survival probability which could be readily compared to experimental data would be also desirable, and these authors provide none.

In a different context, Stein, Peterson, and Fayer through a series of articles[16–19] have developed a spectral overlap model for EET at high temperatures in polymeric glasses and liquids, which provides a quasiquantitative agreement with experimental data obtained by the same authors. However, this model is mainly phenomenological, as it ignores the details of the microscopic transfer processes, due to the difficulties of modeling the interaction of the electronic levels with the phonons and lack of knowledge about the detailed form of the density of phonon states in the systems the authors studied.

For these reasons, in this work we propose a generalization of the aforementioned models in order to account for a general description of the EET dynamics in disordered solids at finite temperatures with inhomogeneously-broadened electronic energy levels. The scope of this work is twofold. Firstly, we present a generalization of the truncated cumulant expansion which can be used to account for the EET in both finite and infinite disordered solids with a distribution of both donor and acceptor energies. Secondly, the expressions so obtained are applied to the simple case where transfer in a disordered, infinite solid involves one phonon, without restricting the energy mismatch of the ions. We find that two quite different temporal regimes emerge where the temperature and energy dependence are quite distinct, even in this simple case. Analytical expressions are presented in the low- and high-temperature limits.

The outline of this work is as follows: in Sec. II we describe the main features of the truncated cumulant expansion method, together with a generalization of this technique to account for an inhomogeneously-broadened distribution of OAI in a disordered solid. In spite of the generality of this method, in order to arrive at analytical expressions for the quantities of interest, which give more physical insight in the problem than *ab initio* numerical modeling of the system, we have explicitly applied it to the simple physical system of an infinite homogeneously-disordered solid. We will show that, even with these simplifying assumptions, we obtain results that apply to real disordered solids. In particular, it will turn out that the survival probability does not only depend on time, but also on temperature and on the energy of the initially excited donor, i.e., the frequency of the pumping source relative to the mean energy of the acceptor distribution. In Sec. III and IV we present the main steps of the calculation of the truncated cumulant expansion taking into account the contribution of one-phonon-assisted processes to the nonresonant EET. In Sec. V, we summarize the main results of the truncated cumulant calculated in the previous sections, and discuss some issues about where the crossover between the two temporal regimes mentioned above should be. Section VI will be devoted to stating the conclusions that can be extracted from this work. Finally, in Appendixes A and B, we present a detailed derivation of the main mathematical results.

II. GENERALIZATION OF THE FIRST-ORDER TRUNCATED CUMULANT EXPANSION METHOD

Electronic energy transfer can be modeled in terms of a quantity, $G^s(t)$, which represents the diagonal part of the Green function solution to the master equation of the system.[10,11] The physical meaning of $G^s(t)$ is the probability that an excitation remains on the initially-excited ion at time t. In fact, this quantity can be readily compared with experimental observables obtained from fluorescence line narrowing (FLN) experiments. Since the time dependence of the observable arises from the spatial distribution of unexcited OAI around the excited ion, namely the acceptors, the ensemble average of $G^s(t)$, which we shall denote $\langle G^s(t)\rangle$, is the quantity measured.

The general expression for $\langle G^s(t)\rangle$, for an initially-excited donor is given by[1]

$$\langle G^s(t)\rangle = \frac{1}{V_d}\int \exp\left\{-c\int [1-p_d(\vec{r}_{da};t)] \times f(\vec{r}_a)\,d\vec{r}_a\right\} f(\vec{r}_d)\,d\vec{r}_d\,. \tag{1}$$

In this expression $p_d(\vec{r}_j,t)$ is the probability of the donor ion being excited at a time t taking into account only the excitation transfer to the acceptor located at site $\vec{r}_a$; $f(\vec{r}_a)$ and $f(\vec{r}_d)$ are the acceptor and donor spatial distribution functions, respectively; V_d is the volume spanned by the donor, and c is the number density of acceptor ions, which verifies the normalization condition $c\int f(\vec{r})d\vec{r}=N-1$, with N the number of OAI in the system.

To arrive at Eq. (1), two main approximations are used.[11] First, the two-particle approximation is introduced, i.e., the excitation decay of the donor ion due to an acceptor located at $\vec{r}_a$ is assumed to be unaffected by the presence of other acceptors. This allows one to reduce the n-particle problem to a superposition of two-particle problems. Second, the cumulant expansion in terms of the number density of OAI is truncated at first order, assuming a very low concentration of OAI.

In the simpler case of an infinite, disordered system, Eq. (1) becomes[10]

$$\ln\langle G^s(t)\rangle = -4\pi c\int [1-p(\vec{r}_{da};t)]r_{da}^2\,dr_{da}\,. \tag{2}$$

For example, for incoherent, resonant dipole-dipole energy transfer[3]

$$p(\vec{r}_{da},t)=\frac{1}{2}\left\{1+\exp\left[-\frac{2t}{\tau}\left(\frac{R_0}{r_{da}}\right)^6\right]\right\} \tag{3}$$

is obtained, where τ is the fluorescence lifetime of the electronic transition involved and R_0 is the critical transfer radius for donor-donor transport (the distance at which the rate of transfer to unexcited OAI is equal to the fluorescence decay rate of the donor in absence of acceptors), and Eq. (2) has the analytical solution[10]

$$\ln\langle G^s(t)\rangle = -\frac{4\pi c}{3}2^{1/2}\left(\frac{t}{\tau}\right)^{1/2}R_0^3\,\Gamma\left(\frac{1}{2}\right), \tag{4}$$

where $\Gamma(x)$ is the gamma function.

It is straightforward to generalize Eq. (1) to account for cases where the transition energy of the acceptor, E_a, and of the donor E_d, vary through the solid, as do the transfer rates

(nonresonant EET), giving rise to an energy mismatch, $\Delta E_{da}=E_d-E_a$, which also varies through the solid. To this end, an additional average over the acceptor and donor transition energies has to be included, leading to an expression for the truncated cumulant expansion given by

$$\langle G^s(t)\rangle=\frac{1}{V_d}\int \exp\left\{-c\int [1-p_d(\Delta E_{da},\vec{r}_{da};t)] \times g(E_a)f(\vec{r}_a)dE_a d\vec{r}_a\right\} g(E_d)f(\vec{r}_d)dE_d\,d\vec{r}_d, \tag{5}$$

where $p_d(\Delta E_{da},\vec{r}_{da};t)$ represents the probability of the initially-excited donor ion with transition energy E_d being excited at time t, taking into account only the interaction with the acceptor ion located at $\vec{r}_{da}$ from donor ion, which has a transition energy E_a. $g(E_a)[g(E_d)]$ is the distribution function of the acceptor (donor) energies.

In the spirit of the two-particle approximation, $p_d(\Delta E_{da},\vec{r}_{da};t)$ can be analytically calculated. To this end, we consider the rate equations

$$\frac{dp_d}{dt}(t)=-w_{da}p_d+w_{ad}p_a, \tag{6}$$

$$\frac{dp_a}{dt}(t)=-w_{ad}p_a+w_{da}p_d, \tag{7}$$

where $w_{da}(w_{ad})$ is the donor$\rightarrow$acceptor (acceptor$\rightarrow$donor) transfer rate, and p_a is the probability of the considered acceptor to be excited. It is easy to see that if the transfer rates depend on T, the probability p_d will also, so we should modify expression (5) to account for this additional parameter.

The previous system can be easily solved by taking into account the detailed balance condition[13]

$$e^{-\beta E_d}w_{da}=w_{ad}e^{-\beta E_a}, \tag{8}$$

to give

$$p_d(\Delta E_{da},T,\vec{r}_{da};t)=\frac{e^{-\beta\Delta E_{da}}}{e^{-\beta\Delta E_{da}}+1}+\frac{e^{-(w_{da}+w_{ad})t}}{e^{-\beta\Delta E_{da}}+1}, \tag{9}$$

$$p_a(\Delta E_{da},T,\vec{r}_{da};t)=\frac{1}{e^{-\beta\Delta E_{da}}+1}-\frac{e^{-(w_{da}+w_{ad})t}}{e^{-\beta\Delta E_{da}}+1}, \tag{10}$$

which after substitution in expression (5) leads to

$$\langle G^s(T;t)\rangle=\frac{1}{V_d}\int \exp\left\{-c\int \frac{1-e^{-(w_{da}+w_{ad})t}}{e^{-\beta\Delta E_{da}}+1} \times g(E_a)\,f(\vec{r}_a)dE_a\,d\vec{r}_a\right\} g(E_d)\,f(\vec{r}_d)\,dE_d\,d\vec{r}_d. \tag{11}$$

In these expressions, $\beta=1/k_BT$, with k_B the Boltzmann constant and T the temperature. It is important to note that we have explicitly indicated a temperature dependence of the cumulant which comes from a possible temperature dependence of the transfer rates.

In the following, we shall restrict ourselves to the simpler situation of an infinite, disordered solid, which is easier to study analytically. In this case, due to translational invariance of the system, if we change the inner integral variable from $\vec{r}_a$ to $\vec{r}_d-\vec{r}_a$, the outer integral over $\vec{r}_d$ gives a factor V_d which cancels the one in the denominator of Eq. (11).

Another simplification that we shall make is to consider that the light which initially excites donor ions is monochromatic, so we can put the distribution of initially excited ions in the form

$$g(E_d)=\delta(E_d-E_0), \tag{12}$$

where E_0 is the energy of the monochromatic incident light.

With these assumptions, Eq. (11) reads

$$\ln\langle G^s(E_0,T;t)\rangle=-4\pi c\int \frac{1-e^{-(w_{da}+w_{ad})t}}{e^{-\beta\Delta E_{da}}+1}g(E_a)\,r_{da}^2\,dE_a\,dr_{da}. \tag{13}$$

Expressions (11) and (13) are the fundamental equations of this work and, in the next section, we shall apply them to a case of special interest: one-phonon-assisted EET, which plays an essential role in the dynamics of the EET at very low temperature.

III. ONE-PHONON PROCESSES CONTRIBUTION TO THE TRUNCATED CUMULANT EXPANSION

The contribution of the one-phonon-assisted processes to the nonresonant EET transfer rate can be calculated very easily by using the Fermi-golden rule in the Debye approximation to give[13]

$$w_{da}=\frac{J^2\gamma^2}{2\pi\rho\Delta E_{da}^2v^5}\int [f(\omega)+1]h(\vec{q},\vec{r}_{da})\omega^3[\delta(\hbar\omega-\Delta E_{da}) +\delta(\hbar\omega+\Delta E_{da})]d\omega, \tag{14}$$

where the notation is as follows: $J=b_n/r_{da}^n$ is the multipolar electrostatic coupling between the ions, where b_n is a constant which depends on the multipolar moments of both ions, and n is the corresponding multipolar exponent ($n=3$ for dipole–dipole interaction, $n=4$ for quadrupole–dipole interaction, and so on); γ is the ion–phonon coupling strength difference between the states involved in the optical transition; ρ is the mass density of the material; v is the sound velocity averaged over orientations; $f(x)=1/(e^{\beta x}-1)$ is the Bose–Einstein distribution function and, finally, $h(\vec{q},\vec{r})=\langle|e^{i\vec{q}\cdot\vec{r}}-1|^2\rangle$ is the so-called coherence factor, where the angle brackets denote average over orientations.

For a disordered solid, where phonons are just acoustic waves, and $\vec{q}$ can take any value, the coherence factor can be evaluated to be

$$h(\vec{q}\cdot\vec{r})=\langle|1-e^{i\vec{q}\vec{r}}|^2\rangle=2\left(1-\frac{\sin qr}{qr}\right), \tag{15}$$

so

$$w_{da}+w_{ad}=\frac{J^2g^2}{\pi\rho\hbar^4v^5}|\Delta E_{da}|\left[1-\frac{\sin\left(\frac{|\Delta E_{da}|r_{da}}{\hbar v}\right)}{\frac{|\Delta E_{da}|r_{da}}{\hbar v}}\right]\times\coth\left(\frac{\beta|\Delta E_{da}|}{2}\right). \tag{16}$$

In the limiting case where the phonons which contribute most to the EET are those with $\vec{q}$ very large, that is, those phonons with very short wavelengths, the coherence factor is approximately 2, and we recover the usual expression for the transfer rate, namely

$$w_{ad}+w_{da}=\frac{J^2\gamma^2|\Delta E_{da}|}{\pi\rho\hbar^4v^5}\coth\left(\frac{\beta|\Delta E_{da}|}{2}\right). \tag{17}$$

The opposite limit consists in assuming that the main contribution to the one-phonon-assisted processes comes from those phonons with very long wavelength compared with the interionic distances, that is, those with very small $\vec{q}$, so we can put $h(\vec{q},\vec{r})\approx q^2r^2/3$.

In this case, the exponent of Eq. (13) is given by

$$w_{da}+w_{ad}=\frac{J^2\gamma^2|\Delta E_{da}|^3r_{da}^2}{6\pi\rho\hbar^6v^7}\coth\left(\frac{\beta|\Delta E_{da}|}{2}\right). \tag{18}$$

In the following, we shall carry out the detailed evaluation of Eq. (13) in the general case. However, it is easy to see from the previous expressions that it is difficult to obtain any analytical result if we take into account the exact expression for the coherence factor, so we have used the very crude approximation of taking the coherence factor as

$$h(qr)=\begin{cases}\frac{1}{3}\left(\frac{|\Delta E_{da}|r}{\hbar v}\right)^2 & \text{if } r<\frac{\sqrt{6}\hbar v}{|\Delta E_{da}|},\\ 2 & \text{otherwise}\end{cases} \tag{19}$$

which resembles the main features of the exact coherence factor, as can be seen in Fig. 1.

Moreover, it is necessary to assume a specific form of the energy distribution function of the acceptor ions, in order to get any physical insight. Therefore, we shall consider a realistic case by assuming that the acceptor energies are distributed according to the Gaussian inhomogeneous profile

$$g(E_a)=\frac{1}{\sigma\sqrt{\pi}}\exp\left[-\left(\frac{E_a-\overline{E}}{\sigma}\right)^2\right], \tag{20}$$

where $\overline{E}$ is the mean energy of the acceptors and σ is the half-width of the distribution.

Let us now consider the evaluation of the averaged cumulant in detail.

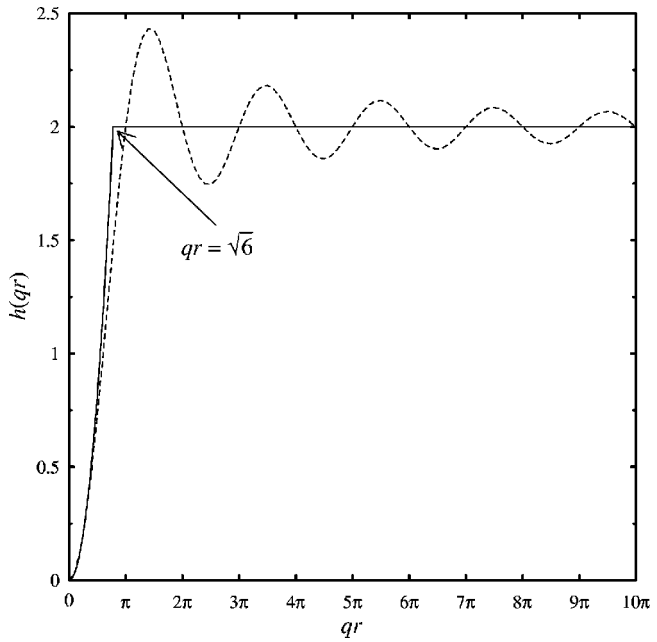

FIG. 1. Coherence factor. The dashed line indicates the exact result for a disordered solid [Eq. (15)], whereas the solid line corresponds to the approximated coherence factor used in this work [Eq. (19)].

IV. EVALUATION OF THE CUMULANT AVERAGE

As stated above, the form of the $(w_{da}+w_{ad})t$ exponent is the one given by expression (16), and we can put it in a more convenient form in order to perform calculations by means of

$$(w_{da}+w_{ad})t=\begin{cases}F(\Delta E_{da},t)/r_{da}^{2n} & \text{if } r_{da}>\sqrt{6}\hbar v/|\Delta E_{da}|\\ F'(\Delta E_{da},t)/r_{da}^{2n'} & \text{otherwise}\end{cases}, \tag{21}$$

where

$$F(\Delta E_{da},t)=\frac{b_n^2\gamma^2}{\pi\rho\hbar^4v^5}t\,|\Delta E_{da}|\coth\frac{\beta|\Delta E_{da}|}{2}, \tag{22}$$

and

$$F'(\Delta E_{da},t)=\frac{b_n^2\gamma^2}{\pi\rho\hbar^6v^7}t\,|\Delta E_{da}|^3\coth\frac{\beta|\Delta E_{da}|}{2}, \tag{23}$$

with $n'=n-1$.

Therefore, the expression we have to evaluate is given by

$$\ln\langle G^s(E_0,T;t)\rangle=-4\pi c\int_0^{\sqrt{6}\hbar v/|\Delta E_{da}|}\frac{1-\exp\left[\frac{F'(\Delta E_{da},t)}{r^{2n'}}\right]}{e^{-\beta\Delta E_{da}}+1}\times g(E_a)\,dE_a\,r^2dr-4\pi c\int_{\sqrt{6}\hbar v/|\Delta E_{da}|}^{R_a}\times\frac{1-\exp\left[\frac{F(\Delta E_{da},t)}{r^{2n}}\right]}{e^{-\beta\Delta E_{da}}+1}g(E_a)\,dE_a\,r^2dr, \tag{24}$$

and once the spatial average is performed (see Appendix A) we arrive at

$$\ln\langle G^s(E_0,T;t)\rangle = -\frac{4\pi}{3}c\int_{-\infty}^{\infty}\frac{F'(\Delta E_{da},t)^{3/2n'}}{e^{-\beta\Delta E_{da}}+1}\times\Gamma\left(1-\frac{3}{2n'},\frac{|\Delta E_{da}|^{2n}F(\Delta E_{da},t)}{(\sqrt{6}\hbar v)^{2n}}\right)\times g(E_a)\,dE_a+\frac{4\pi}{3}c\int_{-\infty}^{\infty}\frac{F(\Delta E_{da},t)^{3/2n}}{e^{-\beta\Delta E_{da}}+1}\times\Gamma\left(1-\frac{3}{2n},\frac{|\Delta E_{da}|^{2n}F(\Delta E_{da},t)}{(\sqrt{6}\hbar v)^{2n}}\right)\times g(E_a)\,dE_a-\frac{4\pi}{3}\Gamma\left(1-\frac{3}{2n}\right)c\times\int_{-\infty}^{\infty}\frac{F(\Delta E_{da},t)^{3/2n}}{e^{\beta\Delta E_{da}}+1}g(E_a)\,dE_a, \quad (25)$$

where $\Gamma(\alpha)$ is the gamma function and $\Gamma(\alpha,z)=\int_z^\infty t^{\alpha-1}e^{-t}dt$ is the incomplete gamma function.

In order to further proceed, we change the integration variable from E_a to $\Delta E_{da}=x$ and introduce the parameters

$$y=\frac{E_0-\overline{E}}{\sigma} \quad (26)$$

and

$$z=\beta\sigma, \quad (27)$$

which will be used through the rest of this work. Also, in order to compare the theory with experimental data, it is preferable to introduce the new parameter combinations

$$R_n=\left(\frac{b_n^2\gamma^2}{\pi\rho\hbar^4v^5}\sigma\tau\right)^{1/2n}, \quad (28)$$

and

$$R_n'=\left(\frac{b_n^2\gamma^2}{6\pi\rho\hbar^6v^7}\sigma^3\tau\right)^{1/2n'}, \quad (29)$$

where τ is the lifetime of the transition involved, and R_n (R_n') has dimensions of a length. In terms of these parameters, and after substitution of $F(\Delta E_{da},t)$, $F'(\Delta E_{da},t)$, and $g(E_a)$ in Eq. (25), we get the form of the cumulant for an infinite disordered solid with an inhomogeneous profile

$$\ln\langle G^s(y,z;t)\rangle = -\frac{4\pi}{3}cR'^3_n\left(\frac{t}{\tau}\right)^{3/2n'}\frac{1}{\sqrt{\pi}}\int_{-\infty}^{\infty}\frac{\left(|x|^3\coth\frac{z|x|}{2}\right)^{3/2n'}}{e^{-zx}+1}\Gamma\left[1-\frac{3}{2n'},\left(\frac{R_n'}{R_n}\right)^{2nn'}\frac{t}{\tau}|x|^{2n+1}\coth\frac{z|x|}{2}\right]e^{-(x-y)^2}dx - \frac{4\pi}{3}cR_n^3\left(\frac{t}{\tau}\right)^{3/2n}\frac{\Gamma\left(1-\frac{3}{2n}\right)}{\sqrt{\pi}}\int_{-\infty}^{\infty}\frac{\left(|x|\coth\frac{z|x|}{2}\right)^{3/2n}}{e^{-zx}+1}e^{-(x-y)^2}dx+\frac{4\pi}{3}cR_n^3\left(\frac{t}{\tau}\right)^{3/2n}\frac{1}{\sqrt{\pi}}\int_{-\infty}^{\infty}\frac{\left(|x|\coth\frac{z|x|}{2}\right)^{3/2n}}{e^{-zx}+1}\times\Gamma\left[1-\frac{3}{2n},\left(\frac{R_n'}{R_n}\right)^{2nn'}\frac{t}{\tau}|x|^{2n+1}\coth\frac{z|x|}{2}\right]e^{-(x-y)^2}dx, \quad (30)$$

It is important to note that we are committing a very small error by extending the integral over negative values of E_a. In real glasses $\overline{E}\sim 10\,000\ \mathrm{cm}^{-1}$ and $\sigma\sim 100\ \mathrm{cm}^{-1}$, so we are extending the integration over energies which are in the very far tale of the Gaussian, and their contributions are very small.

The physical meaning of the radii R_n and R_n' can be easily understood as follows.

By substituting expressions (28), (29), and (19) in Eq. (14), we arrive at

$$w_{da}=\left(\frac{R_n}{r_{da}}\right)^{2n}\frac{\Delta E_{da}}{\sigma}\frac{1}{\tau}, \quad (31)$$

if $r_{da}>\sqrt{6}\hbar v/|\Delta E_{da}|$ and $\Delta E_{da}>0$, and

$$w_{da}=\left(\frac{R_n'}{r_{da}}\right)^{2n'}\left(\frac{\Delta E_{da}}{\sigma}\right)^3\frac{1}{\tau}, \quad (32)$$

if $r_{da}<\sqrt{6}\hbar v/|\Delta E_{da}|$ and $\Delta E_{da}>0$, in the limit $T\to 0$.

Therefore, it turns out that $R_n(R_n')$ stands for the distance, measured from the donor ion, at which the transfer rate to an acceptor ion with energy mismatch $\Delta E_{da}=\sigma$ is equal to the radiative rate at very low temperatures.

This result seems to indicate that we can establish a relation between the radii R_n and R_n', and the Förster critical radius, R_0.

The resonant contribution to the EET is given by the zeroth term in the perturbation chain of the transition rate, i.e., by the terms for which no phonons are created nor destroyed during the optical transition[13]. The contribution of such processes to the transfer rate is given by

$$w_{da}^{(0)}=\frac{2\pi}{\hbar}J_n^2\rho(E_a=E_d), \tag{33}$$

where $\rho(E_a=E_d)$ is the density of acceptor states with the same energy than the donor. This density of states can be stated in terms of the lifetime of the considered transition, by means of

$$\rho(E_a=E_d)=\frac{\tau}{\hbar}, \tag{34}$$

where $\hbar$ is the Planck constant.

In terms of the Förster critical radius, the resonant EET transfer rate is given by

$$w_{da}^{(0)}=\left(\frac{R_0^{(n)}}{r_{da}}\right)^{2n}\frac{1}{\tau}, \tag{35}$$

where $R_0^{(n)}$ is the Förster critical radius for the multipolar interaction of exponent n. By comparing Eq. (33) with (35) we arrive at

$$b_n^2=\frac{\hbar^2}{2\pi}(R_0^{(n)})^{2n}\frac{1}{\tau^2}, \tag{36}$$

which leads, once we take into account this last expression in Eq. (28), to

$$R_n=R_0^{(n)}\left(\frac{\gamma^2\sigma}{2\pi^2\rho\hbar^2v^5\tau}\right)^{1/2n}, \tag{37}$$

and from the relation between the two radius introduced in this model,

$$R_n'=\left(\frac{\sigma R_n^n}{\sqrt{6}\hbar v}\right)^{1/n'}, \tag{38}$$

we can calculate the values of R_n and R_n' in terms of the Förster critical radius.

If we take a value of $\sigma\approx100\ \mathrm{cm}^{-1}$, $\gamma\approx1000\ \mathrm{cm}^{-1}$, $\tau\approx1$ ms, $v\approx1000$ m/s, and $\rho\approx1000\ \mathrm{kg/m}^3$, we get

$$R_3\approx0.01\,R_0, \tag{39}$$

for dipole–dipole interaction which, for a value $R_0\approx100$ Å gives $R_3\approx1$ Å and $R_3'\approx0.877$ Å.

Another important point is to evaluate the long and short time limits of Eq. (30). In the short-time limit, i.e., $t/\tau\ll1$, the incomplete Gamma function $\Gamma(\alpha,x)$ approaches to the Gamma function $\Gamma(x)$, so Eq. (30) reduces to

$$\ln\langle G^s(y,z;t)\rangle=-\frac{4\pi}{3}\Gamma\left(1-\frac{3}{2n'}\right)\frac{R_n'^3c}{\sqrt{\pi}}\left(\frac{t}{\tau}\right)^{3/2n'}\times\int_{-\infty}^{\infty}\frac{\left(|x|^3\coth\frac{z|x|}{2}\right)^{3/2n'}}{e^{-zx}+1}e^{-(x-y)^2}\,dx. \tag{40}$$

In the opposite limit, $t/\tau\gg1$, the incomplete Gamma function tends to zero, so Eq. (30) reduces to

$$\ln\langle G^s(y,z;t)\rangle=-\frac{4\pi}{3}\Gamma\left(1-\frac{3}{2n}\right)\frac{R_n^3c}{\sqrt{\pi}}\left(\frac{t}{\tau}\right)^{3/2n}\times\int_{-\infty}^{\infty}\frac{\left(|x|\coth\frac{z|x|}{2}\right)^{3/2n}}{e^{-zx}+1}e^{-(x-y)^2}\,dx. \tag{41}$$

To quote an example, for a dipole–dipole interaction, expressions (40) and (41) have $(t/\tau)^{3/4}$ and $(t/\tau)^{1/2}$ temporal dependences, respectively.

It is interesting to consider the low- and high-temperature behavior of the long- and short-time limits expressions, which we do in the next sections.

A. Long-time limit

In the high-temperature limit $z\ll1(k_BT\gg\sigma)$, we can make a series expansion in powers of z of the temperature dependent part of the integrand in Eq. (41), and retain only the lowest term of the expansion, and we arrive at (see Appendix B)

$$\ln\langle G^s(y,z;t)\rangle\approx-\frac{4\pi}{3}R_n^3\Gamma\left(1-\frac{3}{2n}\right)c\left(\frac{t}{\tau}\right)^{3/2n}\frac{2^{-1+3/2n}}{z^{3/2n}}. \tag{42}$$

In the low-temperature limit, $z\gg1(k_BT\gg\sigma)$, we use continuous fraction expansions in terms of e^{-zx}, and arrive at

$$\ln\langle G^s(y,z;t)\rangle\approx-\frac{4\pi}{3}R_n^3c\frac{1}{2\sqrt{\pi}}\Gamma\left(1-\frac{3}{2n}\right)\left(\frac{t}{\tau}\right)^{3/2n}e^{-y^2}\times\left\{\Gamma\left(\frac{1}{2}+\frac{3}{4n}\right)H_{3/2n}^1(y)+\frac{3}{n}\frac{\Gamma\left(\frac{3}{2n}\right)}{z^{1+3/2n}}\times\left[\frac{3}{n}+4\left(\frac{9}{4n^2}-1\right)\frac{y}{z}\right]\right\}, \tag{43}$$

where

$$H_{3/2n}^1(y)=\Phi\left(\frac{1}{2}+\frac{3}{4n},\frac{1}{2};y^2\right)+\frac{3}{2n}y\frac{\Gamma\left(\frac{3}{4n}\right)}{\Gamma\left(\frac{1}{2}+\frac{3}{4n}\right)}\times\Phi\left(1+\frac{3}{4n},\frac{3}{2};y^2\right), \tag{44}$$

with $\Phi(\alpha,\beta;x)$ the confluent hypergeometric functions.[20]

In the limit of very small y, the function $H_{3/2n}^1(y)$ is very well-described by the series expansion

$$H_{3/2n}^1(y)\approx1+\frac{3}{2n}\frac{\Gamma\left(\frac{3}{4n}\right)}{\Gamma\left(\frac{1}{2}+\frac{3}{4n}\right)}y, \tag{45}$$

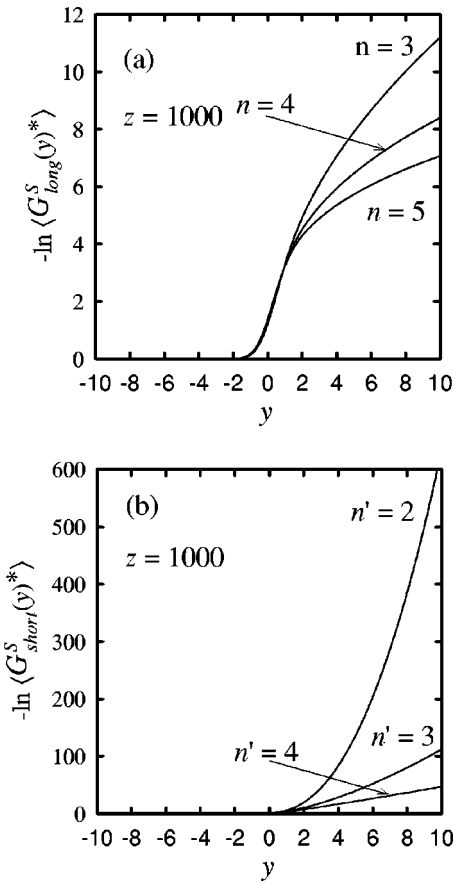

FIG. 2. Cumulant expansion dependence on the laser frequency at very low temperatures: (a) long-time limit [Eq. (43)], for dipole–dipole ($n=3$), dipole–quadrupole ($n=4$), and quadrupole–quadrupole ($n=5$); (b) short-time limit [Eq. (50)], for dipole–dipole ($n'=2$), dipole–quadrupole ($n'=3$), and quadrupole–quadrupole ($n'=4$).

which is easier to compare to experimental data.

The y-dependence of the low-temperature limit cumulant expansion can be seen in Fig. 2(a) for various multipolar interactions.

To quote an example, expression (41) for $n=3$ (dipole–dipole interaction) reduces to

$$\ln\langle G^s(y,z;t)\rangle = -\frac{4\pi}{3}R_3^3 c\left(\frac{t}{\tau}\right)^{1/2} \times \int_{-\infty}^{\infty} \frac{\left(|x|\coth\frac{z|x|}{2}\right)^{1/2}}{e^{-zx}+1} e^{-(x-y)^2}\,dx. \tag{46}$$

The high-temperature limit is given by

$$\ln\langle G^s(y,T;t)\rangle = -\frac{4\pi}{3}R_3^3 c\sqrt{\frac{\pi}{2}}\left(\frac{t}{\tau}\right)^{1/2}\left(\frac{k_BT}{\sigma}\right)^{1/2}, \tag{47}$$

and the low-temperature limit is given by

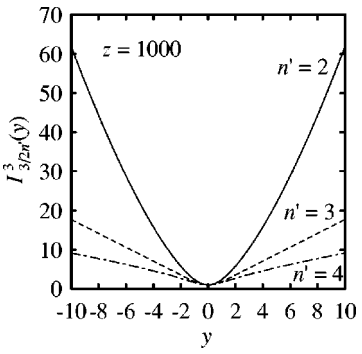

FIG. 3. Short time limit cumulant expansion dependence on the laser frequency at very high temperatures [Eq. (49)], for dipole–dipole ($n'=2$), dipole–quadrupole ($n'=3$), and quadrupole–quadrupole ($n'=4$).

$$\ln\langle G^s(y,T;t)\rangle \approx -\frac{4\pi}{3}R_3^3 c\frac{1}{2}\left(\frac{t}{\tau}\right)^{1/2} e^{-y^2}\left\{\Gamma\left(\frac{3}{4}\right)H^1_{1/2}(y) + \Gamma\left(\frac{1}{2}\right)\left[\left(\frac{k_BT}{\sigma}\right)^{3/2} - 3y\left(\frac{k_BT}{\sigma}\right)^{5/2}\right]\right\}, \tag{48}$$

with $H^1_{1/2}(y)=\Phi(\frac{3}{4},\frac{1}{2};y^2)+y/2[\Gamma(\frac{1}{4})/\Gamma(\frac{3}{4})]\Phi(\frac{5}{4},\frac{3}{2};y^2)$ or $H^1_{1/2}(y)\approx 1+\frac{1}{2}[\Gamma(\frac{1}{4})/\Gamma(\frac{3}{4})]y$ in the small y-limit.

B. Short-time limit

In the high-temperature limit, $z\ll 1$, the cumulant is given by (Appendix B)

$$\ln\langle G^s(y,z;t)\rangle \approx -\frac{4\pi}{3}R'^3_n c\Gamma\left(1-\frac{3}{2n'}\right)\Gamma\left(\frac{1}{2}+\frac{3}{4n'}\right) \times\left(\frac{t}{\tau}\right)^{3/2n'} I^3_{3/2n'}(y)\frac{2^{-1+3/2n'}}{\sqrt{\pi}z^{3/2n'}}, \tag{49}$$

where $I^3_{3/2n'}(y)=e^{-y^2}\Phi(\frac{1}{2}+3/2n',\frac{1}{2};y^2)$ or, for small y, $I^3_{3/2n'}(y)\approx 1+3/n'y^2$.

The behavior of $I^3_{3/2n'}(y)$ can be seen in Fig. 3 for some multipolar interactions.

In the low-temperature limit, $z\gg 1$, the cumulant is given by

$$\ln\langle G^s(y,z;t)\rangle \approx -\frac{4\pi}{3}R'^3_n c\Gamma\left(1-\frac{3}{2n'}\right)\frac{1}{2}\left(\frac{t}{\tau}\right)^{3/2n'} \times e^{-y^2}\left\{\Gamma\left(\frac{1}{2}+\frac{9}{4n'}\right)H^3_{3/2n'}(y) + \frac{9}{n'}\frac{\Gamma\left(\frac{9}{2n'}\right)}{z^{1+9/2n'}}\left[\frac{3}{n'}+4\left(\frac{3}{2n'}-1\right) \times\left(1+\frac{9}{2n'}\right)\frac{y}{z}\right]\right\}, \tag{50}$$

where

$$H^3_{3/2n'}(y)=\Phi\left(\frac{1}{2}+\frac{9}{4n'},\frac{1}{2};y^2\right)+\frac{9}{2n'}y\frac{\Gamma\left(\frac{9}{4n'}\right)}{\Gamma\left(\frac{1}{2}+\frac{9}{4n'}\right)}\times\Phi\left(1+\frac{9}{4n'},\frac{3}{2};y^2\right). \quad (51)$$

In the small y-limit

$$H^3_{3/2n'}(y)\approx 1+\frac{9}{2n'}\frac{\Gamma\left(\frac{9}{4n'}\right)}{\Gamma\left(\frac{1}{2}+\frac{9}{4n'}\right)}y. \quad (52)$$

The frequency dependence of the truncated cumulant in this limit can be seen in Fig. 2(b) for some multipolar interactions.

For dipole–dipole interaction ($n=3\rightarrow n'=2$), the general expression of the cumulant is given by

$$\ln\langle G^s(y,z;t)=-\frac{4\sqrt{\pi}}{3}\Gamma\left(\frac{1}{4}\right)R'^3_3 c\left(\frac{t}{\tau}\right)^{3/4}\times\int_{-\infty}^{\infty}\frac{\left(|x|^3\coth\frac{z|x|}{2}\right)^{3/4}}{e^{-zx}+1}e^{-(x-y)^2}dx. \quad (53)$$

The high-temperature limit is given by

$$\ln\langle G^s(y,T;t)\rangle\approx-\frac{4\pi}{3}R'^3_3\frac{\Gamma\left(\frac{1}{4}\right)^2}{2^{9/4}\sqrt{\pi}}\left(\frac{t}{\tau}\right)^{3/4}I^3_{3/4}(y)\left(\frac{k_BT}{\sigma}\right)^{3/4}, \quad (54)$$

with $I^3_{3/4}(y)=e^{-y^2}\Phi(\frac{5}{4},\frac{1}{2};y^2)$, or $I^3_{3/4}(y)\approx 1+\frac{3}{2}y^2$, whereas the low-temperature limit is given by

$$\ln\langle G^s(y,T;t)\rangle\approx-\frac{4\pi}{3}R'^3_3 c\frac{\Gamma\left(\frac{1}{4}\right)}{2\sqrt{\pi}}\left(\frac{t}{\tau}\right)^{3/4}e^{-y^2}\times\left\{\Gamma\left(\frac{13}{18}\right)H^3_{3/4}(y)+\frac{9}{2}\Gamma\left(\frac{9}{4}\right)\left[\frac{3}{2}\left(\frac{k_BT}{\sigma}\right)^{13/4}-\frac{13}{4}y\left(\frac{k_BT}{\sigma}\right)^{17/4}\right]\right\}, \quad (55)$$

with

$$H^3_{3/4}(y)=\Phi\left(\frac{13}{8},\frac{1}{2};y^2\right)+\frac{9}{4}y\frac{\Gamma\left(\frac{9}{8}\right)}{\Gamma\left(\frac{13}{8}\right)}\Phi\left(\frac{17}{8},\frac{3}{2};y^2\right),$$

or

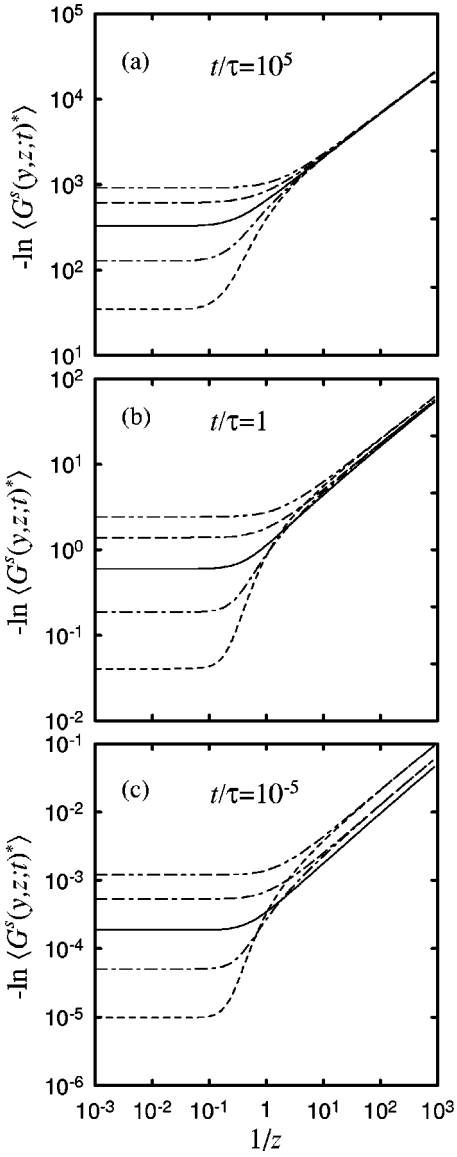

FIG. 4. Temperature dependence of the numerically-evaluated truncated cumulant [Eq. (30)] for various times and laser frequencies. (Solid line) $y=0.0$; $(----)$ $y=-1.0$; $(-\cdot-\cdot-)$ $y=-0.5$; $(--\cdot--)$ $y=0.5$; $(--\cdot\cdot--)$ $y=1.0$. (a) $t/\tau=10^5$; (b) $t/\tau=1$; (c) $t/\tau=10^{-5}$.

$$H^3_{3/4}(y)\approx 1+\frac{9}{4}\frac{\Gamma\left(\frac{9}{8}\right)}{\Gamma\left(\frac{13}{8}\right)}y$$

for small y.

V. RESULTS FOR THE DIPOLE–DIPOLE INTERACTION CASE AND DISCUSSION

In this section we will present the analysis of the results found in the previous section for the case of dipole–dipole interaction which is, by far, the most important case from an experimental point of view.

In Fig. 4 we can see the temperature dependence of the truncated cumulant for fixed laser frequencies and delay times. It is important to note that in the rest of the figures of this work, the quantity represented is not the logarithm of the

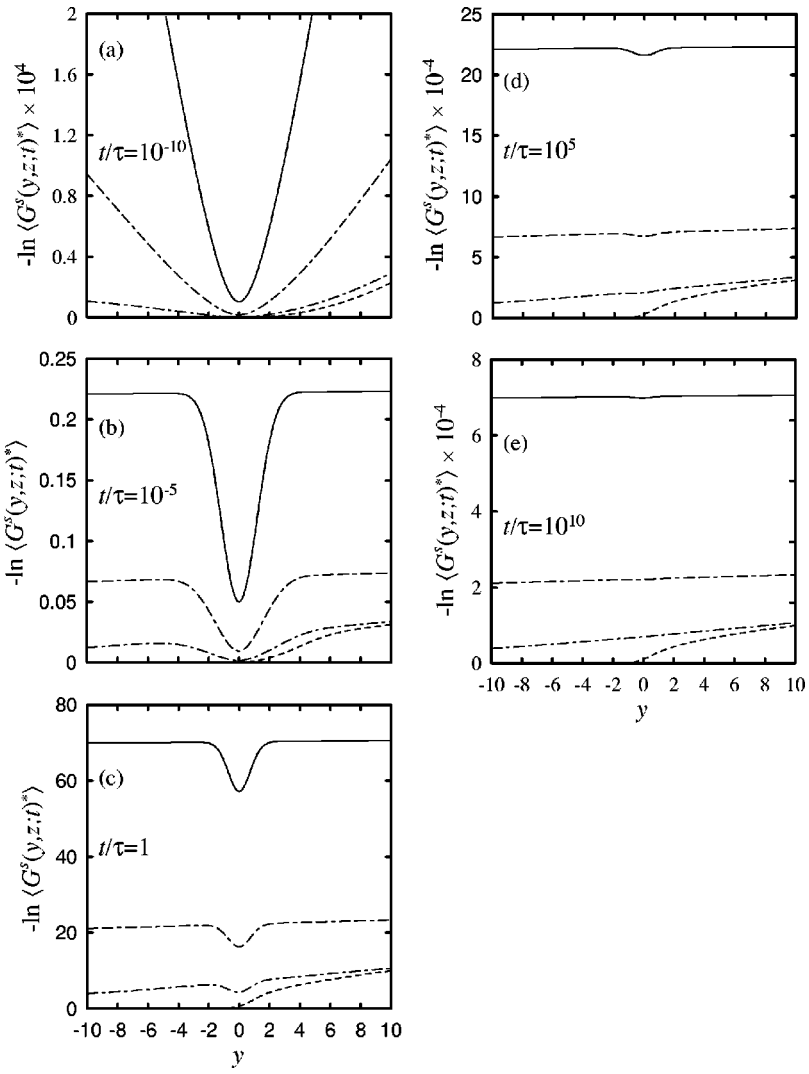

FIG. 5. Laser frequency dependence of the numerically-evaluated truncated cumulant for different times and temperatures [Eq. (30)]. (Solid line) $z=0.001$;$(--\cdot--)$ $z=0.01$; $(-\cdot-\cdot-)$ $z=0.1$; $(----)$ $z=1000$. (a) $t/\tau=10^{-10}$; (b) $t/\tau=10^{-5}$; (c) $t/\tau=1$; (d) $t/\tau=10^{5}$; (e) $t/\tau=10^{10}$.

cumulant, but this quantity divided by the factor $(4\pi/3\sqrt{\pi}c)$, which gets rid of the unknown quantity c. We indicate this fact by using the notation $\langle G^s(t)^*\rangle$, instead of $\langle G^s(t)\rangle$.

The first important feature we note in that figure is that the cumulant is nearly constant up to $k_BT\approx\sigma$. This fact makes us consider what is the relative importance of the one-phonon processes contribution to the EET at very low temperatures, which will be discussed below.

Furthermore, we can note some of the main features predicted in the previous section. For example, we can see from expressions (48) and (55) that the functions $H_k^m(y)$ are nonsymmetric in y. However, in the high temperature limit [Eqs. (47) and (54)], the cumulant is symmetric on y. Moreover, it does not depend on y in the long time limit. All these features can be noted in Fig. 4.

In Fig. 5 we have plotted the laser frequency dependence of the cumulant for fixed temperatures and delay times. We can see in that figure how the behavior changes from the one given by Eqs. (54) and (55) at short times to the one predicted by Eqs. (47) and (48) at long times, respectively, passing through an intermediate regime which can be well-described only by numerical evaluation of the truncated cumulant.

In Fig. 6 we present the delay time dependence of the truncated cumulant for fixed temperatures and laser frequencies. We can see how the slope of the curves changes from a $(t/\tau)^{3/4}$ at very short times to a $(t/\tau)^{1/2}$ at long times.

One point of crucial importance is where such a crossover occurs. In fact, this point can be estimated, at $y=0$, as follows:

Let us consider expression (30) for $y=0$. In the following discussion, it will be useful to introduce the following notation:

$$\ln\langle G^s_{\rm short}(z;t)\rangle = -\frac{4\pi}{3}cR'^3_n\left(\frac{t}{\tau}\right)^{3/2n'}\frac{1}{\sqrt{\pi}} \times\int_{-\infty}^{\infty}\frac{\left(|x|^3\coth\frac{z|x|}{2}\right)^{3/2n'}}{e^{-zx}+1} \times\Gamma\left[1-\frac{3}{2n'},\left(\frac{R'_n}{R_n}\right)^{2nn'} \times\frac{t}{\tau}|x|^{2n+1}\coth\frac{z|x|}{2}\right]e^{-x^2}\,dx, \quad (56)$$

and

$$\ln\langle G^s_{\rm long}(z;t)\rangle = -\frac{4\pi}{3}cR_n^3\left(\frac{t}{\tau}\right)^{3/2n} \times\frac{\Gamma\left(1-\frac{3}{2n}\right)}{\sqrt{\pi}}\int_{-\infty}^{\infty}\frac{\left(|x|\coth\frac{z|x|}{2}\right)^{3/2n}}{e^{-zx}+1}e^{-x^2}dx + \frac{4\pi}{3}cR_n^3\left(\frac{t}{\tau}\right)^{3/2n}\frac{1}{\sqrt{\pi}}\int_{-\infty}^{\infty}\frac{\left(|x|\coth\frac{z|x|}{2}\right)^{3/2n}}{e^{-zx}+1} \times\Gamma\left[1-\frac{3}{2n},\left(\frac{R_n'}{R_n}\right)^{2nn'} \times\frac{t}{\tau}|x|^{2n+1}\coth\frac{z|x|}{2}\right]e^{-x^2}dx. \quad (57)$$

The index ''short'' makes reference to the fact that $\langle G^s_{\rm short}(z;t)\rangle$ is responsible for the 3/4 temporal dependence at very short times, whereas the ''long'' index makes reference to the fact that $\langle G^s_{\rm long}(z;t)\rangle$ is responsible for the 1/2 temporal dependence at long times. The second term in $\langle G^s_{\rm long}(z;t)\rangle$ is a correction to the $t^{1/2}$ decay. Again, by using an asterisk superscript, we will mean that the corresponding function is divided by $(4\pi/3\sqrt{\pi})c$.

By using the procedure described in Appendix B, we can develop low and high temperature expansions of these functions for short- and long-time limits. The results of such expansions are summarized in Table I.

At very low temperatures, $\langle G^s_{\rm long}(z;t)\rangle$ changes from t/τ to a $(t/\tau)^{1/2}$ dependence at

$$\frac{t_1}{\tau}=0.67\left(\frac{R_3}{R_3'}\right)^{12}, \quad (58)$$

whereas $\langle G^s_{\rm short}(z;t)\rangle$ changes from a $(t/\tau)^{3/4}$ to a $(t/\tau)^{2/7}$ dependence at

$$\frac{t_2}{\tau}=0.047\left(\frac{R_3}{R_3'}\right)^{12}. \quad (59)$$

Therefore, the delay time at which the dominant contribution changes from $\langle G^s_{\rm short}(z;t)\rangle$ to $\langle G^s_{\rm long}(z;t)\rangle$, that is, the point at which $\langle G^s_{\rm short}(z;t)\rangle$ and $\langle G^s_{\rm long}(z;t)\rangle$ become the same, is given by

$$\frac{t_0}{\tau}=0.18\left(\frac{R_3}{R_3'}\right)^{12}. \quad (60)$$

In the high-temperature limit, we can make an analogous analysis, from which we obtain that $\langle G^s_{\rm long}(z;t)\rangle$ changes from t/τ to a $(t/\tau)^{1/2}$ dependence at

$$\frac{t_1}{\tau}=1.23\left(\frac{R_3}{R_3'}\right)^{12}z, \quad (61)$$

and $\langle G^s_{\rm short}(z;t)\rangle$ changes from $(t/\tau)^{3/4}$ to $(t/\tau)^{2/7}$ at

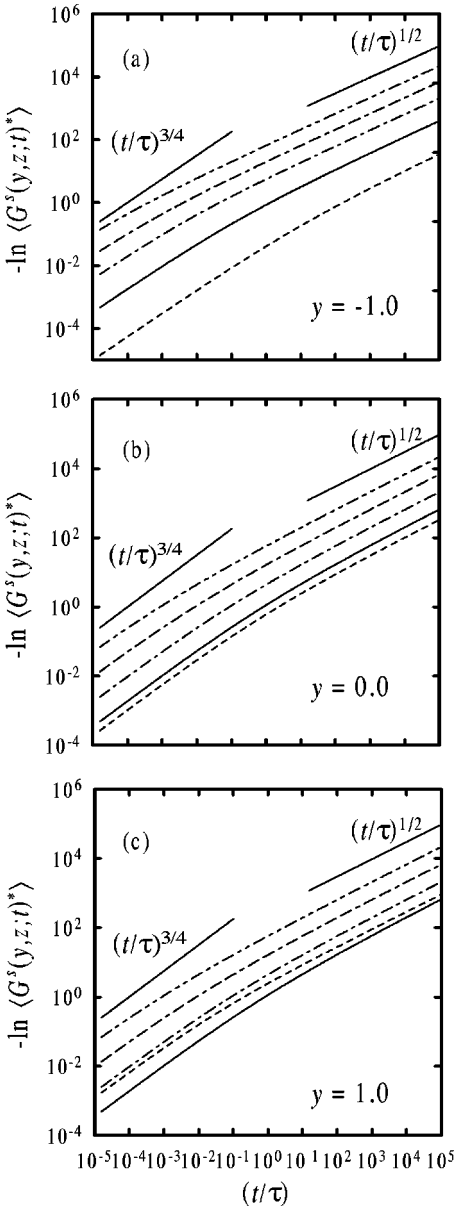

FIG. 6. Temporal dependence of the numerically-evaluated truncated cumulant for various temperatures and laser frequencies [Eq. (30)] for $R_3=1$ Å. $(----)$ $z=1000$; (Solid line) $z=1$; $(-\cdot-\cdot-)$ $z=0.1$; $(--\cdot--)$ $z=0.01$; $(-\cdot\cdot-\cdot\cdot-)$ $z=0.001$. (a) $y=-1.0$; (b) $y=0.0$; (c) $y=1.0$. The asymptotic temporal dependences $(t/\tau)^{1/2}$ and $(t/\tau)^{3/4}$ are shown for comparison.

$$\frac{t_2}{\tau}=0.035\left(\frac{R_3}{R_3'}\right)^{12}z,$$

and the delay time at which $\langle G^s_{\rm long}(z;t)\rangle$ and $\langle G^s_{\rm short}(z;t)\rangle$ become the same is given by

$$\frac{t_0}{\tau}=0.20\left(\frac{R_3}{R_3'}\right)^{12}z.$$

In Fig. 7 we have summarized these results in the very low and very high temperature limits for $R_3=1$ Å. As can be seen, the agreement with the above results is astonishingly good. These simple ideas predict very well where the

TABLE I. Limiting behaviors of $\langle G^s_{\rm short}(z;t)^*\rangle$ and $\langle G^s_{\rm long}(z;t)^*\rangle$ at $y=0$.

Temperature range	Time range	$-\log\langle G^s_{\rm long}(z;t)^*\rangle$	$-\log\langle G^s_{\rm short}(z;t)^*\rangle$
$z\gg 1$	$\frac{t}{\tau}\ll\left(\frac{R_3}{R'^3}\right)^{12}$	$\frac{3}{4}\sqrt{\pi}\frac{R'^6_3}{R^3_3}\frac{t}{\tau}$	$\frac{1}{2}\Gamma(\frac{1}{4})\Gamma(\frac{13}{8})R'^3_3\left(\frac{t}{\tau}\right)^{3/4}$
	$\frac{t}{\tau}\gg\left(\frac{R_3}{R'^3}\right)^{12}$	$\frac{\sqrt{\pi}}{2}\Gamma(\frac{3}{4})R^3_3\left(\frac{t}{\tau}\right)^{1/2}$	$\frac{4}{13}\Gamma(\frac{5}{7})\frac{R_3^{39/7}}{R'^{18/7}_3}\left(\frac{t}{\tau}\right)^{2/7}$
$z\ll 1$	$\frac{t}{\tau}\ll\left(\frac{R_3}{R'^3}\right)^{12}$	$2\frac{R'^6_3}{R^3_3}\frac{t}{\tau z}$	$\frac{\Gamma(\frac{1}{4})^2}{2^{9/4}}R'^3_3\left(\frac{t}{\tau}\right)^{3/4}$
	$\frac{t}{\tau}\gg\left(\frac{R_3}{R'^3}\right)^{12}$	$\frac{\pi}{\sqrt{2}}R^3_3\left(\frac{t}{\tau z}\right)^{1/2}$	$\frac{2^{4/3}}{5}\Gamma(\frac{2}{3})\frac{R^5_3}{R'^2_3}\left(\frac{t}{\tau z}\right)^{1/3}$

numerically calculated curves change their slope, and can be used as a guide of where we should see a crossover, even for small departures from $y=0$.

As commented above, an important question is what is the relative importance of resonant EET when both types of transfer, resonant and nonresonant, are present in the solid. In order for the resonant transfer to have a noticeable effect, the two ions involved must have transition frequencies that differ by no more than 1 or 2 times the homogeneous linewidth. Therefore, the resonant EET is not important in disordered systems as long as $\sigma\gg\gamma_H$, where γ_H is the homogeneous linewidth. If this condition is satisfied, it is very unlikely that one will have two ions in the same region of the sample whose transition frequencies differ by an amount $\lesssim\gamma_H$. In this case, one should be able to neglect resonant EET in comparison with non resonant phonon assisted EET.

Another important point is that resonant EET does not affect the decay of the narrow line in FLN experiments, since the width of the narrow line is $\sim\gamma_H$ (assuming the spectrum of the exciting line is a delta function). Thus, the one-phonon calculation without resonant EET should describe the narrow line decay at low temperatures even in the presence of significant resonant EET.

At temperatures of the order of σ, the two-phonon process contribution begins to be important, and it could be expected that there are deviations from the predictions of this model. However, the exact behavior of the two phonon contribution is beyond the scope of this work.

VI. CONCLUSIONS

In this article, the incoherent nonresonant EET between chromophores in disordered solids has been addressed. A generalization of the truncated cumulant expansion method,

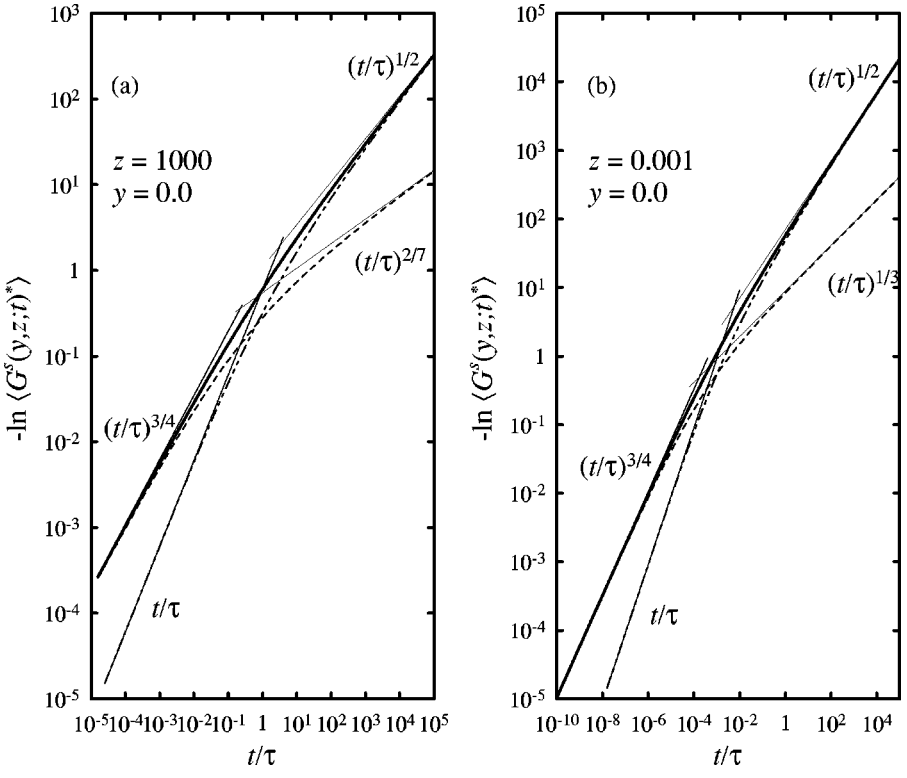

FIG. 7. Analysis of the change of the slope in the temporal dependence of the truncated cumulant for $y=0$. (Heavy solid line) $-\ln\langle G^s(z;t)^*\rangle$; (– – – –) $-\ln\langle G^s_{\rm short}(z;t)^*\rangle$; (– · · – · · –) $-\ln\langle G^s_{\rm long}(z;t)^*\rangle$. The light solid lines represent the asymptotic behaviors of $\langle G^s_{\rm short}(z;t)^*\rangle$ and $\langle G^s_{\rm long}(z;t)^*\rangle$ discussed in Sec. V. (a) $z=1000$; (b) $z=0.001$.

developed earlier, has been introduced in order to account for the inhomogeneously-broadened electronic levels observed in these materials.

The method has been applied to the simple case of an infinite, disordered solid, at very low temperatures, where one-phonon processes dominate the dynamics of the EET.

The quantity which emerges from this calculation, the truncated cumulant, represents the probability that an initially-excited donor is excited at a later time t, and is the observable measured in FLN experiments. This quantity depends not only on time, but also on the energy of the initially-excited donor and on temperature.

The exact behavior of the cumulant has been evaluated, as well as the behavior in the low and high temperature limits, which are stated in terms of the inhomogenous width of the acceptor energy distribution. We find that, in this model, two temporal regimes emerge, where the temperature and initially-excited donor energy dependences are quite distinct. For a dipole–dipole interaction between the OAI, the temporal dynamics of the cumulant has a $t^{3/4}$ dependence at very short times, whereas at long times a $t^{1/2}$ behavior is predicted. The crossover between these behaviors has been also analyzed.

Finally, we would like to stress that this model could be also useful in obtaining structural information from restricted geometries, such as the ones which are characteristic of the energy transfer in biological systems. However, in this type of system, resonant EET may make an important contribution to the measured survival probability, and both types of processes, resonant and nonresonant ones, have to be taken into account in order to describe the experimental results. Thus, the present model should be generalized to include both mechanisms in order to properly describe EET in such systems, which will be the subject of further investigations.

ACKNOWLEDGMENTS

Angel García Adeva would like to acknowledge the Spanish MEC for supporting this work, under the Subprograma General de Perfeccionamiento de Doctores en el Extranjero.

APPENDIX A: EVALUATION OF THE SPATIAL AVERAGE

The spatial average in Eq. (13) can be performed in the following way:

The first summand gives a contribution

$$
\begin{aligned}
&-4\pi c\int_0^{R_a}\frac{g(E_a)}{e^{-\beta\Delta E_{da}}+1}dE_a r_a^2\,dr_a\\
&=-\frac{4\pi}{3}R_a^3 c\int\frac{g(E_a)}{e^{-\beta\Delta E_{da}}+1}dE_a\\
&=-(N-1)\int\frac{g(E_a)}{e^{-\beta\Delta E_{da}}+1}dE_a,
\end{aligned}
\tag{A1}
$$

where R_a is a cutoff radius necessary in order to avoid divergence of the integral.

The second term gives a contribution

$$
\begin{aligned}
&4\pi c\int\frac{g(E_a)}{e^{-\beta\Delta E_{da}}+1}dE_a\int_0^{R_a}e^{-(w_{da}+w_{ad})t}r^2\,dr\\
&=4\pi c\int\frac{g(E_a)}{e^{-\beta\Delta E_{da}}+1}dE_a\\
&\times\left\{\int_0^{u(\Delta E_{da})}e^{-F'(\Delta E_{da},t)/r^{2n'}}r^2\,dr\right.\\
&\left.+\int_{u(\Delta E_{da})}^{R_a}e^{-F(\Delta E_{da},t)/r^{2n}}r^2\,dr\right\},
\end{aligned}
\tag{A2}
$$

with $u(\Delta E_{da})=\sqrt{6}\hbar v/|\Delta E_{da}|$ which, after substitution of $F(\Delta E_{da},t)/r_{da}^{2n}=x$ and $F'(\Delta E_{da},t)/r_{da}^{2n'}=x$, can be put in the form

$$
\begin{aligned}
&\frac{4\pi c}{2n'}\int\frac{F'(\Delta E_{da},t)^{3/2n'}g(E_a)}{e^{-\beta\Delta E_{da}}+1}dE_a\\
&\times\int_{F'(\Delta E_{da},t)/u(\Delta E_{da})^{2n'}}^{\infty}\frac{e^{-x}}{x^{1+3/2n'}}dx\\
&+\frac{4\pi c}{2n}\int\frac{F(\Delta E_{da},t)^{3/2n}g(E_a)}{e^{-\beta\Delta E_{da}}+1}dE_a\\
&\times\int_{F(\Delta E_{da},t)/u(\Delta E_{da})^{2n}}^{F(\Delta E_{da},t)/R_a^{2n}}\frac{e^{-x}}{x^{1+3/2n}}dx,
\end{aligned}
\tag{A3}
$$

After integrating once by parts, and taking into account that

$$
\int_{x_{\min}}^{x_{\max}}x^{-3/2n}e^{-x}\,dx=\Gamma\left(1-\frac{3}{2n},x_{\min}\right)-\Gamma\left(1-\frac{3}{2n},x_{\max}\right),
\tag{A4}
$$

the spatial average gives

$$
\begin{aligned}
&\frac{4\pi}{3}cF(\Delta E_{da},t)^{3/2n}\left[\left(\frac{F(\Delta E_{da},t)}{R_a}\right)^{-3/2n}-\Gamma\left(1-\frac{3}{2n}\right)\right.\\
&\left.+\Gamma\left(1-\frac{3}{2n},\frac{F(\Delta E_{da},t)}{u(\Delta E_{da})^{2n}}\right)\right]-\frac{4\pi}{3}cF'(\Delta E_{da},t)^{3/2n'}\\
&\times\Gamma\left(1-\frac{3}{2n'},\frac{F(\Delta E_{da},t)}{u(\Delta E_{da})^{2n}}\right).
\end{aligned}
\tag{A5}
$$

To arrive to this expression, the limit $x_{\min}\to 0$, that is, $R_a\to\infty$, and the relation $F(\Delta E_{da},t)/u(\Delta E_{da})^{2n}=F'(\Delta E_{da},t)/u(\Delta E_{da})^{2n'}$ have been used.

Substituting expression (A5) in (A3) we obtain

$$(N-1)\int \frac{g(E_a)}{e^{-\beta\Delta E_{da}}+1}dE_a+\frac{4\pi}{3}c\int \frac{F(\Delta E_{da},t)^{3/2n'}g(E_{a)}}{e^{-\beta\Delta E_{da}}+1}$$
$$\times\Gamma\left(1-\frac{3}{2n},\frac{F(\Delta E_{da},t)}{u(\Delta E_{da})^{2n}}\right)dE_a-\frac{4\pi}{3}c$$
$$\times\int \frac{F'(\Delta E_{da},t)^{3/2n'}g(E_{a)}}{e^{-\beta\Delta E_{da}}+1}\Gamma\left(1-\frac{3}{2n'},\frac{F(\Delta E_{da},t)}{u(\Delta E_{da})^{2n}}\right)$$
$$\times dE_a-\frac{4\pi}{3}c\Gamma\left(1-\frac{3}{2n}\right)\int \frac{F(\Delta E_{da},t)^{3/2n}g(E_{a)}}{e^{-\beta\Delta E_{da}}+1}dE_a, \tag{A6}$$

and the first summand exactly cancels the term in (A1), leaving us with Eq. (25).

APPENDIX B: HIGH- AND LOW-TEMPERATURE LIMITS

In order to evaluate the high- and low-temperature limits, we are faced with integrals of the form

$$\int_{-\infty}^{\infty}\frac{\left(|x|^m\coth\frac{z|x|}{2}\right)^k}{e^{-zx}+1}e^{-(x-y)^2}dx, \tag{B1}$$

where $m=1$ and $k=3/2n$ for very long times, and $m=3$ and $k=3/2(n-1)$ in the opposite limit, where n is the order of the multipolar interaction.

In the high temperature limit, $z\ll 1$, we can make a series expansion of the temperature dependent part of the integrand in terms of z. To the lowest order in z

$$\frac{\left(|x|^m\coth\frac{z|x|}{2}\right)^k}{e^{-zx}+1}\approx 2^{k-1}\frac{|x|^{k(m-1)}}{z^k}, \tag{B2}$$

so we are faced with the integral

$$\frac{2^{k-1}}{z^k}\int_{-\infty}^{\infty}|x|^{k(m-1)}e^{-(x-y)^2}dx$$
$$=\frac{2^{k-1}}{z^k}\Gamma\left(\frac{1}{2}+\frac{k(m-1)}{2}\right)I_k^m(y), \tag{B3}$$

where

$$I_k^m(y)=e^{-y^2}\Phi\left(\frac{1}{2}+\frac{k(m-1)}{2},\frac{1}{2};y^2\right), \tag{B4}$$

where $\Phi(\alpha,\beta,x)$ denotes the confluent hypergeometric function.[20]

It is important to note that the integral (B3) converges provided that $k(m-1)>-1$, which holds for any multipolar interaction ($n>=3$).

For $m=1$ and $k=3/2n$, Eq. (B3) reads

$$\Gamma\left(\frac{1}{2}\right)\frac{2^{-1+3/2n}}{z^{3/2n}}, \tag{B5}$$

and, after substituting in Eq. (41) we arrive at Eq. (42).

For $m=3$ and $k=3/2n'$, Eq. (B3) reads

$$\Gamma\left(\frac{1}{2}+\frac{3}{2n'}\right)\frac{2^{-1+3/2n'}}{z^{3/2n'}}I^3_{3/2n'}(y), \tag{B6}$$

with $I^3_{3/2n'}(y)=e^{-y^2}\Phi(\frac{1}{2}+3/2n',\frac{1}{2};y^2)$, and, after substitution in Eq. (40), we arrive at Eq. (54).

In the low-temperature limit $z\gg 1(k_BT\ll\sigma)$, it is convenient to express the integral in the following way:

$$\int_{-\infty}^{\infty}\frac{\left(|x|^m\coth\frac{z|x|}{2}\right)^k}{e^{-zx}+1}e^{-(x-y)^2}dx$$
$$=\int_0^{\infty}\left(x^m\coth\frac{zx}{2}\right)^k e^{-(x-y)^2}dx$$
$$-2e^{-y^2}\int_0^{\infty}\frac{\left(x^m\coth\frac{zx}{2}\right)^k}{e^{zx}+1}\sinh(2xy)e^{-x^2}dx. \tag{B7}$$

By using the continuous fraction expansions

$$\left(\coth\frac{zx}{2}\right)^k\approx 1+2ke^{-zx}, \tag{B8}$$

$$\frac{\left(\coth\frac{zx}{2}\right)^k}{e^{zx}+1}\approx e^{-zx}, \tag{B9}$$

where only the lowest power of z has been retained, after making the transformation $x\to x/z$ we arrive at

$$\int_0^{\infty}x^{mk}e^{-(x-y)^2}dx+2k\frac{e^{-y^2}}{z^{1+mk}}\int_0^{\infty}x^{mk}e^{-x}e^{2xy/z}dx$$
$$-2y\frac{y}{z^{1+mk}}e^{-y^2}\int_0^{\infty}x^{mk}e^{-x}\sinh\frac{2xy}{z}e^{-x^2}dx, \tag{B10}$$

which, to the lowest order in z gives

$$\frac{1}{2}\Gamma\left(\frac{1+mk}{2}\right)e^{-y^2}H_k^m(y)+mk\Gamma(mk)\frac{e^{-y^2}}{z^{1+mk}}\Big[2k+4(k-1)$$
$$\times(1+mk)\frac{y}{z}\Big], \tag{B11}$$

where

$$H_k^m(y)=\Phi\left(\frac{1+mk}{2},\frac{1}{2};y^2\right)$$
$$+mky\frac{\Gamma\left(\frac{mk}{2}\right)}{\Gamma\left(\frac{1+mk}{2}\right)}\Phi\left(\frac{2+mk}{2},\frac{3}{2};y^2\right). \tag{B12}$$

For $m=1$ and $k=3/2n$ we get

$$e^{-y^2}\left\{\frac{1}{2}\Gamma\left(\frac{1}{2}+\frac{3}{4n}\right)H^1_{3/2n}(y)+\frac{3}{2n}\frac{\Gamma\left(\frac{3}{2n}\right)}{z^{1+3/2n}}\left[\frac{3}{n}+4\left(\frac{9}{4n^2}-1\right)\frac{y}{z}\right]\right\}, \quad \text{(B13)}$$

with

$$H^1_{3/2n}(y)=\Phi\left(\frac{1}{2}+\frac{3}{4n},\frac{1}{2};y^2\right)+\frac{3}{2n}y\frac{\Gamma\left(\frac{3}{4n}\right)}{\Gamma\left(\frac{1}{2}+\frac{3}{4n}\right)}\Phi\left(1+\frac{3}{4n},\frac{3}{2};y^2\right), \quad \text{(B14)}$$

and, after a little algebra, we arrive at Eq. (43).

For $m=3$ and $k=3/2n'$ we get

$$e^{-y^2}\left\{\frac{1}{2}\Gamma\left(\frac{1}{2}+\frac{9}{4n'}\right)H^3_{3/2n'}(y)+\frac{9}{2n'}\frac{\Gamma\left(\frac{9}{2n'}\right)}{z^{1+9/2n'}}\times\left[\frac{3}{n'}+4\left(\frac{3}{2n'}-1\right)\left(\frac{9}{2n'}+1\right)\frac{y}{z}\right]\right\}, \quad \text{(B15)}$$

with

$$H^3_{3/2n'}(y)=\Phi\left(\frac{1}{2}+\frac{9}{4n'},\frac{1}{2};y^2\right)+\frac{9}{2n'}y\frac{\Gamma\left(\frac{9}{4n'}\right)}{\Gamma\left(\frac{1}{2}+\frac{9}{4n'}\right)}\times\Phi\left(1+\frac{9}{4n'},\frac{3}{2};y^2\right), \quad \text{(B16)}$$

and we arrive at Eq. (50).

[1] D.M. Hussey, S. Matzinger, and M.D. Fayer, J. Chem. Phys. **109**, 8708 (1998).
[2] P.T. Rieger, S.P. Palese, and R.J. Dwayne Miller, Chem. Phys. **221**, 85 (1997).
[3] Th. Förster, Ann. Phys. (Leipzig) **2**, 55 (1948).
[4] D.L. Huber, D.S. Hamilton, and B. Barnett, Phys. Rev. B **16**, 4642 (1977).
[5] W.Y. Ching, D.L. Huber, and B. Barnett, Phys. Rev. B **17**, 5025 (1978).
[6] D.L. Huber and W.Y. Ching, Phys. Rev. B **18**, 5320 (1978).
[7] D.L. Huber, Phys. Rev. B **20**, 2307 (1979).
[8] D.L. Huber, Phys. Rev. B **20**, 5333 (1979).
[9] C.R. Gochanour, H.C. Andersen, and M.D. Fayer, J. Chem. Phys. **70**, 4254 (1979).
[10] K.A. Peterson and M.D. Fayer, J. Chem. Phys. **85**, 4702 (1986).
[11] A.H. Marcus and M.D. Fayer, J. Chem. Phys. **94**, 5622 (1991).
[12] S.W. Haan and R. Zwanzig, J. Chem. Phys. **68**, 1879 (1978).
[13] T. Holstein, in *Laser Spectroscopy of Solids*, edited by W.M. Yen and P.M. Selzer (Springer-Verlag, Berlin, 1986).
[14] I.R. Martín, V.D. Rodríguez, I.R. Martín, and U.R. Rodríguez-Mendoza, Phys. Rev. B **57**, 3396 (1998).
[15] V. Lavín, I.R. Martín, U.R. Rodríguez-Mendoza, and V.D. Rodríguez, J. Phys.: Condens. Matter **11**, 8739 (1999).
[16] A.D. Stein, K.A. Peterson, and M.D. Fayer, Chem. Phys. Lett. **161**, 16 (1989).
[17] A.D. Stein, K.A. Peterson, and M.D. Fayer, J. Chem. Phys. **92**, 5622 (1990).
[18] A.D. Stein, K.A. Peterson, and M.D. Fayer, Chem. Phys. Lett. **176**, 159 (1991).
[19] A.D. Stein, and M.D. Fayer, J. Chem. Phys. **97**, 2948 (1992).
[20] I.S. Gradshteyn and I.M. Ryzhik, *Table of Integrals, Series, and Products*, edited by Alan Jeffrey (Academic, New York, 1996).